Silicon (2022) 14:10187–10198
https://doi.org/10.1007/s12633-022-01828-y

REVIEW PAPER

Recent Study on Schottky Tunnel Field Effect Transistor for Biosensing Applications

P Anusuya[1] · Prashanth Kumar[1] · Papanasam Esakki[1] · Lucky Agarwal[1]

Received: 28 January 2022 / Accepted: 8 March 2022 / Published online: 24 March 2022
© The Author(s), under exclusive licence to Springer Nature B.V. 2022

Abstract
In this review, we discussed highly sensitive biosensor devices which is having a more attractive, wide scope and development in the sensing field. Biosensor devices can detect the charged and neutral charged biomolecules such as protein, nucleic acids, antibody agents and viruses. Due to these highly sensitive biosensor devices, we mainly focused on schottky tunnel field-effect transistors (STFET), these transistors have unique properties such as enhanced transconductance and gate controllability, low leakage current etc. In addition, we studied the performances and challenges of STFET by dielectric modulation doping concentration, dielectric modulation, and heterostructure devices. Further, we have reviewed the comparison of STFET and conventional devices. This article reviews mainly on the study of high sensitivity analysis of STFET and modified Schottky-TFET structures for the use of biosensing applications.

Keywords Schottky · Biomolecules · Biosensors · Numerical simulation

1 Introduction

In recent times biosensor-based devices are promising and shows rapid growth in biosensing applications. A biosensor is a typical device due to which the biomolecule interactions are converted into an electrical signal by a transducer. It can detect the bacteria, viruses of the human body and chemical bonds in the biomolecules. Field Effect Transistors are usually incorporated in biosensor devices, which have mainly been used because of their unique properties such as label-free detection, high sensitivity, flexibility, simple, inexpensive, fast, specificity in detection and effectiveness [1–5]. Furthermore, it has some limits where it is unable to detect the charged biomolecules and slow response time. The FET biosensor requires a rapid, robust, low thermal budget, high doping concentration to achieve high sensitivity. To improve the qualities of sensors researcher's focus on the metal oxide semiconductor field-effect transistor in biosensor devices. Usually, MOSFET has high sensitivity, miniaturisation, and quick response time for detection of both charged and neutral charge biomolecules even though it has some issues [6–11]. When scaling down the device it is affected by Short Channel Effects (SCE), power consumption, restrained subthreshold swing, high leakage current [12, 13]. To mitigate these issues researchers proposed schottky tunnel field-effect transistors. Due to their high drive current, high sensitivity, low ambipolar conduction, and low leakage current we demonstrate reliable, specific, rapid STFET biosensors for the detection of biomolecules [14, 15]. It relies on both thermionic emission and the Band-To-Band tunnelling mechanism due to these mechanisms enhanced the performance in terms of high I_{on}/I_{off} ratio. Furthermore, STFET enhances the cut-off frequency and decrease intrinsic delay which increases the speed of the device, [16–21]. Moreover, the major behaviour of biosensing devices is to sense the sensitivity by variation of dielectric constant and charge density methods are considered in STFET [14]. This review mainly reports a comprehensive analysis and performance of STFET devices for biosensing applications. We also discuss novel structures, performances, characteristics compared with conventional devices.

✉ Prashanth Kumar
prash.034@gmail.com

[1] Microelectronics and VLSI Design Group, School of Electronics, VIT-Chennai University, Chennai, Tamil Nadu 600127, India

2 Metallic and Semiconductor Contact-Based Biosensors

Biosensors are sensing tools which are consists of bioreceptor, transducer, and signal processing unit [22]. Biosensors can be

divided into two categories. Physical biosensors (the physical property of medium got the information from the sensing device e.g., sense of hearing, touch and sight) and chemical biosensors (chemical property of medium got the information from the sensing device e.g., sense of smell and taste). Furthermore, the physical biosensors can be classified into optical biosensors or mechanical biosensors as well as chemical biosensors can be classified into electrochemical or biochemical biosensors. In optical biosensor devices, biomolecules interact with light and sensing by an optical transducer system. An optical transducer system can be utilized as surface plasma on resonance (SPR), localized surface plasma on resonance, evanescent wave fluorescence and optical waveguide interferometry. Due to their enhanced performance, they can use for biosensing applications [23–25]. For mechanical biosensor devices, owing to their biomolecule's interaction the surface of the cantilever shifted towards up or down and sense the bioreceptors. Owing to the excellent merits like high sensitivity, quick response time it can be used in biosensing applications. In the electrochemical biosensors, electrode surface structure determined the signal transfer and performance of the device with bio element interactions. The qualitative performance provides high sensitivity, more specific biosensor devices. Figure 1 shows biochemical biosensors convert the biochemical reaction changes into physical signals through the transducer. It provides more specific, reproducible, rapid biosensor devices [27–30]. The different kinds of devices have unique properties to analyze the biomolecules.

3 Fabrication Techniques

Scaling the device is affected by SCEs and other circumstances. To overcome these issues, the device takes a variety of steps taken in fabrication in Oxidation, deposition, etching, patterning, annealing, and ion implantation techniques used in the fabrication of a device.

In 2021, A. Ramos et al. used chemical vapour deposition to create a pseudo-MOSFET of ZnO sheets. Due to high-quality thin films that are extremely pleasant, simple to use, and inexpensive. The CVD process enhanced the device's potential and produced high-quality samples. It was discovered that the band was bending unfavourably. During the CVD procedure, certain flaws occur in the SiO_2/Si substrates. The reaction raises the V_{GS} voltage, resulting in poor crystallinity and a worse ZnO layer transition [31]. Figure 2 shows the chemical vapour deposition process for zinc oxide. The length and width of the channel for ZnO is 1000 μm and 100 μm Au deposited on the silicon substrate.

Andreas Hierlemann, fabricated the sputtering method of the MOSFET device for biosensor applications. The Al deposition (sputtering) can detect the breast cancer antigens using polymeric layers or FPW based immunoassay in the gas state. Next, the etching process provide the membrane structure to the device and again deposited the zinc oxide. Here the IDT process leads to evaporate or depositing the Al or Au. Finally coating the polymers by spray, then biomolecules deposited on the device [32]. Shadab Rabbani et al. proposed a

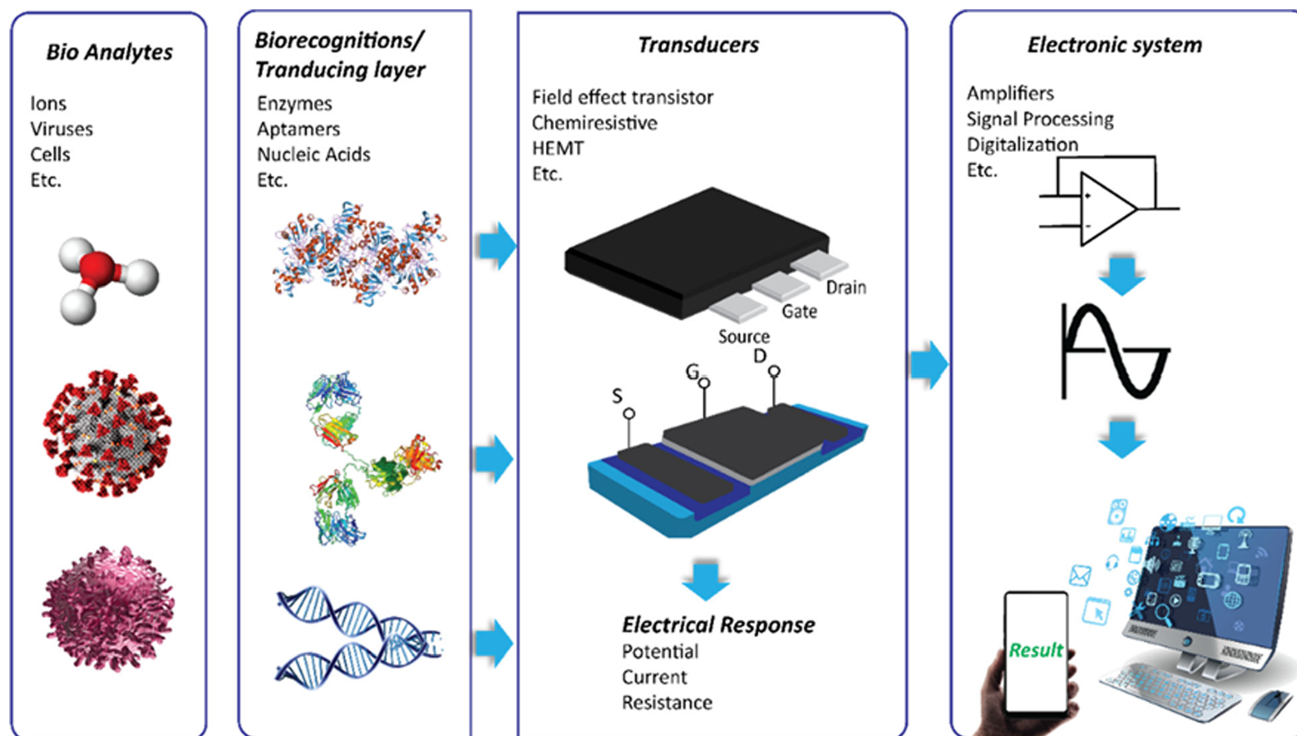

Fig. 1 Schematic diagram of biosensing process [26]

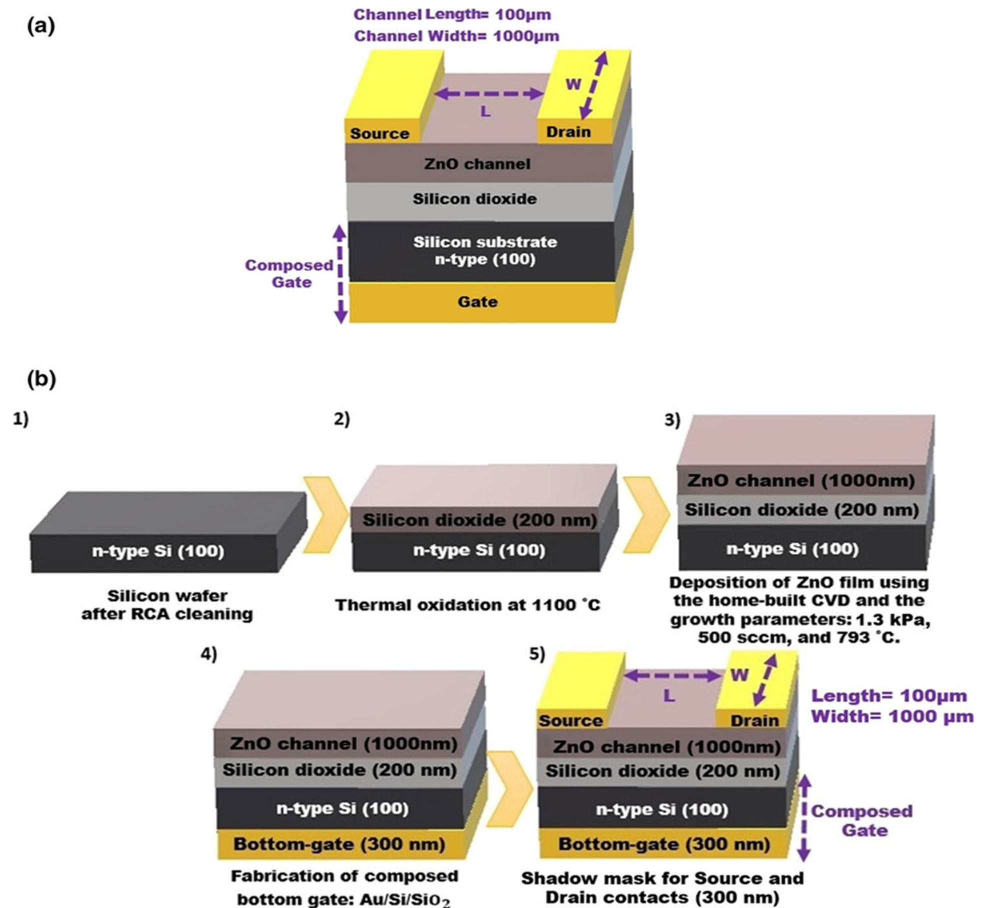

Fig. 2 Schematic process of CVD method [31]

cantilever embedded MOSFET. Using sol-gel process the PZT layer is deposited on the wafer. PZT converts electrical into mechanical energy. The mechanical vibrations lead to the generation of charges and the potential to change the drain current, which is capable to recognize the bio-receptors of the MOSFET device. The parallel array operation and suppressed cantilever length improve the sensitivity of the device [33].

The JL-MOSFET device fabricated by Ajay et al. with recess etching process the nanocavity is formed from source and drain regions. When the SiO_2 layer deposit in the device the biomolecules are influenced by the potential in the channel of the nanocavity region. Which can detect the DNA, enzymes, cells etc. Different structures explained by Namrata Mendiratta et al. based on the MOSFET device [34].

Yu pan et al. in 2019 developed novel monolayer MoS_2 film on a silicon substrate of Fin-FET device using CVD method at low temperature. The low temperature is not affected by STI or Fin structure. MoS_2 FIN-FET device consists of 10 nm length of the back gate, length of the channel is 3 µm, the width of the channel is 45 µm, SiO_2 thickness is 120 nm, and height of the Si fin is 113 nm. This device decreases the leakage current, SiO_2 of the interface layer decrease the lattice mismatching effect in between high-K and Si materials. This device provides high potential, proper switching properties with drain current and excellent electrical properties [35].

Qingzhu Zhang et al. developed a Fin-FET device in 2018. The Si nanowire is used for this device. Because of their properties such as large surface-to-volume ratio and high compatibility with the sputtering technique the spacer is formed. The electrodes length extracted about 2 mm will reduce the leakage current when sensing mesenchymal stem cells. Figure 3 shows one of the physical vapour deposition and in the solid-state, the atoms are oxidized with ions. This leads to control of the film growth. The excellent features it can be used for ultra-sensitive cell-based devices and therapy techniques [37]. Hung-Cheng Lin et al. expressed micro/nanowire Fin-FET device using sol-gel technique in 2015. This technique using for dielectric in capacitors and it provides dielectric properties. A mixture of particles settled on the surface of the layer by Fig. 4. The surface to volume ratio must be large, which can enhance the sensitivity of the device particularly nanowire-based Fin-FET devices. IGZO is prepared for better electrical properties such as low SS, improved threshold voltage and high electron mobility of DUV laser with the decreasing temperature of the annealing process like 600 °C, 450 °C to 300 °C the mobility increases. The mobility ratios are 2, 7 and 56 respectively without the DUV device. Due to the

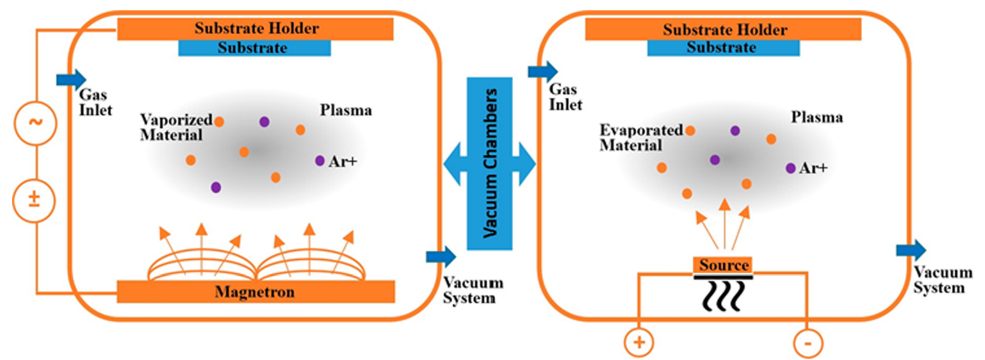

Fig. 3 Schematic process of the sputtering method [36]

homogeneous distribution the mobility of electrons increases. Owing to the device properties can be used in biomedical sensor applications [39].

Tsung- Yang Liow et al. demonstrated n- channel Fin-FET device in the year 2009. Which is using the recess etching technique to well device performances in the channel region. It controls the thickness of the oxide, suppresses the parasitic, SDE resistance and negligible the potential problems hence the I_{DSAT} and strain are improved, which can use in biomedical applications [40].

Chen Chong et al. designed the DMTFET device in the year 2021. The CVD technique (N^+ doping) to achieve excellent performances, with DMTFET device we can detect charge density for positively and negatively charged biomolecules. The charge density range of about 10^{10} cm^{-2} to 10^{13} cm^{-2} has high sensitivity than the other FET devices. I_{on}/I_{off} ratio and SS also improved for this device with good features we can use for biosensing applications [41].

Yan Wu et al. in the year 2017 developed an Mg/Si TFET used RF magnetron sputtering technique. Multi-stacks of Mg/Si films are formed by a sputtering method, which leads to an annealing process and an n-Si interface layer formed on the substrate provides excellent electrical properties of the device [42].

Deepika Singh et al. in the year 2016 exposed Dielectric Modulated Junction-less TFET using charge plasma technique to detect the biomolecules. The Fabrication method is the simple and lesser thermal budget required, due to this steeper SS and I_{on}/I_{off} ratio are investigated to sense the biomolecules. Hence the sensitivity performance is high than the MOSFET devices [43].

Anran Gao et al. exposed robust silicon nanowire Tunnel-FET biosensor. Figure 5 represented the first layer of the semiconductor material over the second material layer and when annealing the compound at a specific temperature, the metal contact is evaporating. The wet etching technique used for the TFET device with SiNW can provide high controllability. Further, it generates the smooth and maximum quality due to the minimum size, well cross-section, and maximum surface fictionalization. Depending on the variation of analyte binding, n and p channel devices operated. SiNW TFET is capable to provide high sensitivity when compared to SiNW FET device leads to sensing applications of POC diagnostics [45].

Sebastian Preg et al. developed the SB-NW-FET device in the year 2013. With the CVD technique, electrical properties are improved. SB-NW-FET having tunneling mechanism for carrier transport, using the thermal oxidation hysteresis was removed and gate potential controlled the ambipolar conduction. Moreover, the output characteristics show high on- current about 1.6 mA. The parallel arrays show hysteresis and unipolar p-type behavior, which leads to achieving better performance for biosensing applications. [46].

Qianqian Huang et al. in the year 2011 demonstrated self-depleted T- gate STFET using sputtering technique. Improved the thermal stability of NiSi by Ni sputtering. Using this method the SS behavior is decreased and improved the drive current, better saturation behavior and decreases the parasitic resistance [47].

Louis Hutin et al. in the year 2016 developed SBTFET using the Ge enrichment technique. SiGe thin film is formed is about 11 nm and metal/high-k dielectric materials are deposited and patterned. The drain and source regions are grown using ion implantation and anneal spike on the gate. Using the

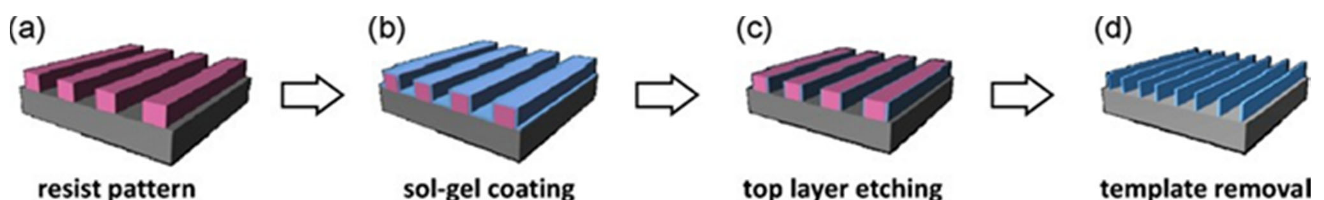

Fig. 4 Schematic process of sol-gel process [38]

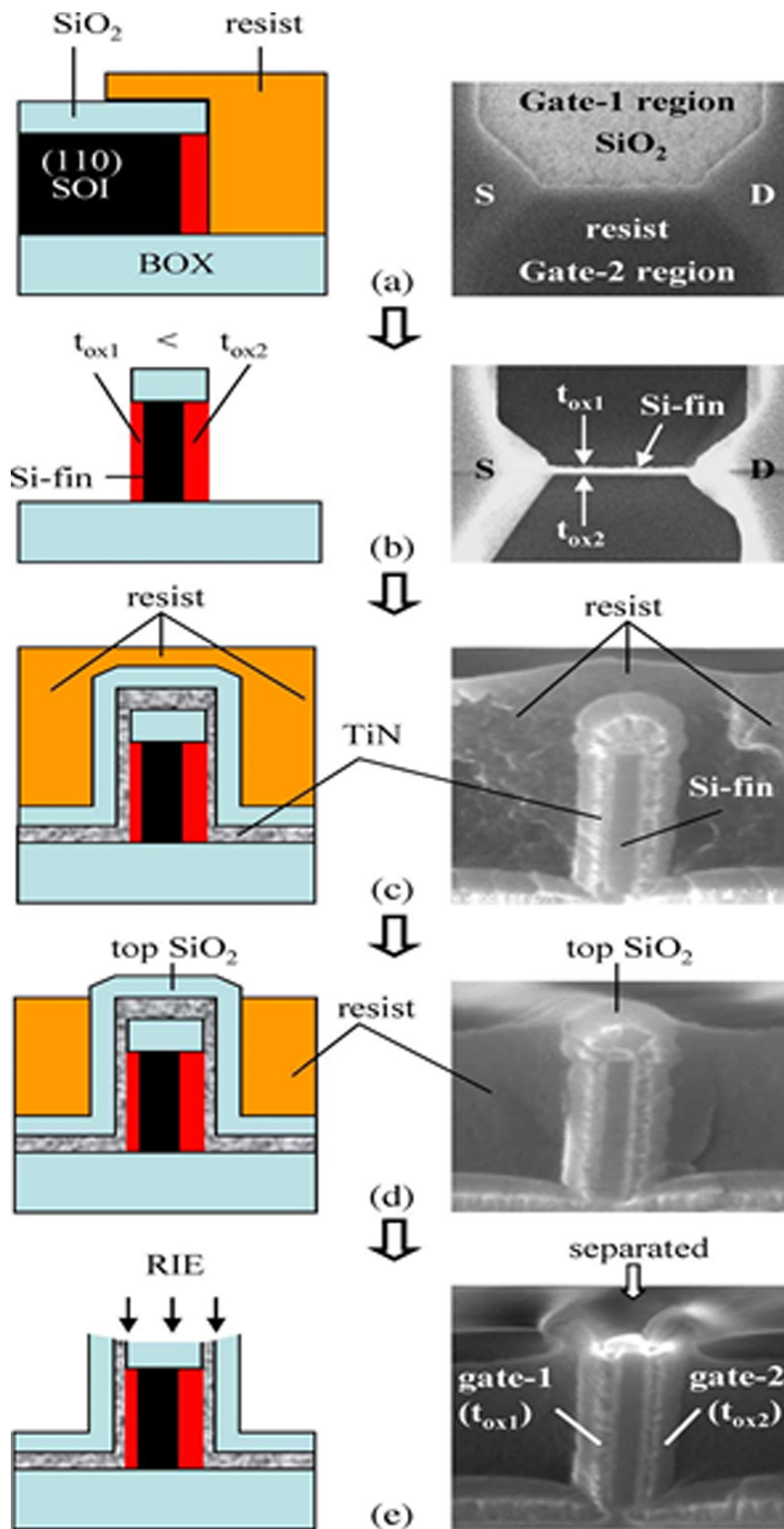

Fig. 5 Schematic process of recess etching technique [44]

SBTFET device decreases leakage currents and ambipolar conduction [48].

Sangeeta Sing et al. in the year 2016 fabricated Self-aligned charge plasma STFET using lithography and ion implantation technique. Hence the device provides steeper SS, reduced SCEs and ambipolar conduction because of these features is used as bio and opto compatible applications [49].

Usually, schottky contact is obtained in between the CNT and metal electrodes. Owing to schottky contact transfer the charges between the electrodes of the device. Schottky contact-based materials are palladium, gold, platinum, titanium and molybdenum used for the CNT BioFET device. Karnaushenko et al provided CNT based BioFET with schottky contact in the year 2015. The thermal annealing process offers to suppress the barrier width, charge transmission is improved due to the schottky contact shown in Table 1. [50]

4 Performance of the STFET Device

Parameters are important for the performance of the device. The parameters determine qualitative and quantitative electrical characteristics (surface potential, electric field, permittivity, sensitivity) and modified structures (length, width, gate materials) of the device. In the CP-SB-TEFT device, varying the work function, as a result, suppress the SCEs, leakage current, SS and the Fig. 6 shows when varying the gate-source voltage, the drain current obtained for different drain, source, a double, doped pocket of CP-SB-TFET and variation of different drain-source voltages as a result maximum drain current observed at 1.2 V. The change in work function increases and decrease the tunneling probability is obtained and variation of gate-source voltage for a different work function, provides maximum drain current observed for a work function of 3.9 eV by Fig. 7. The variation of pocket thickness leads to enhanced the SS, DIBL, V_{TH} and I_{ON} to the CP-SB-TFET device. The oxide thickness decreases, on- state current increases. In channel length variation not more affects the device performance, but when silicon thickness decreases, gate controllability and on-current increases [51].

4.1 Dielectrically modulated STFET devices

Double pocket doped ferroelectric SB tunnel FET device exhibits the enhanced drive current, transconductance, gate controllability, I_{on}/I_{off} ratio, and suppress the ambipolar conduction, subthreshold swing because of the tunneling width is reduces in the Ioff state, low FE layer thickness, zero fields relative permittivity, negative capacitance, doping at both regions (source and drain) and interface region of the channel. So, it improved the device performance by Sangeeta Singh et al. and Shilpi Guin et al. [16, 52]. SB-TFET does not occur in-between the p-source and channel region when compared to Doping-Less TFET [53]. SB-

Table 1 Different techniques for STFET based devices [46–50]

S.No	Device	Method	Purpose
1	SB-NW-FET	CVD technique	Control the ambipolar conduction
2	T- gate STFET	sputtering technique	Good saturation behaviour, increase thermal stability, reduces parasitic resistance
3	SBTFET	Ge enrichment technique	Suppress leakage and ambipolar conduction
4	Self-aligned charge plasma STFET	lithography and ion implantation technique	Reduces short channel effects, leakage, ambipolar conduction

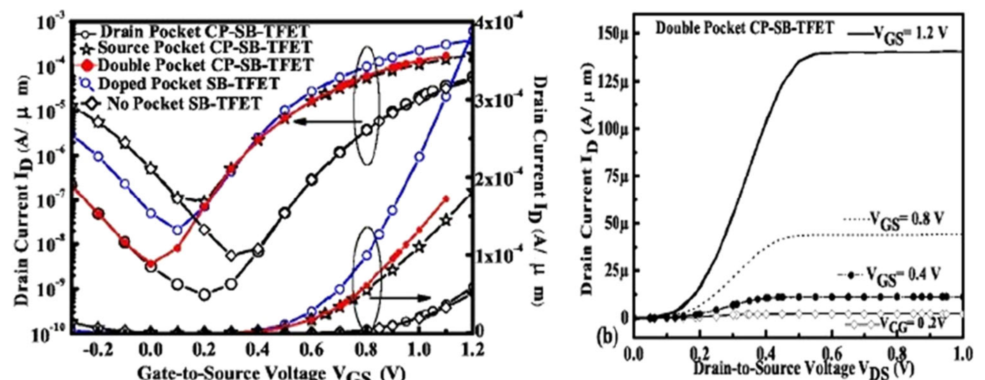

Fig. 6 Transfer and output characteristics of CP-SBFET for different devices at $V_{GS} = 1$ V [51]

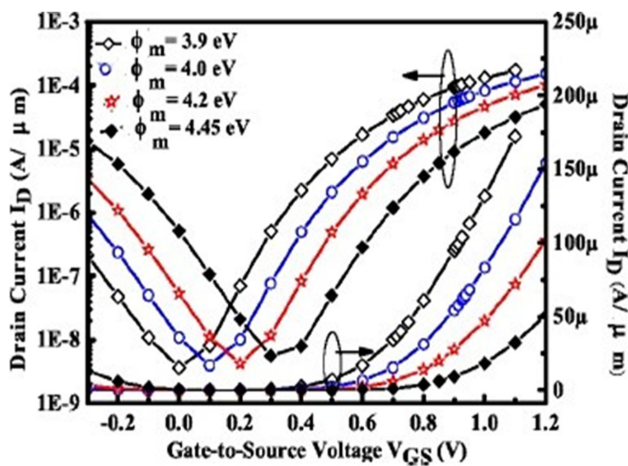

Fig. 7 Different Work functions for CP-SBTFET [51]

TFET occur between the metal source and channel region [54], which leads to suppressing the random dopant fluctuations. This results in good electrical properties of the DM-SBTFET device, which can be used as biosensor applications. Further, different gate metal workfunction is considered to improve the gate controllability of the device show in Table 2.

4.2 Junctionless STFET devices

Instead of P-N junction the JL techniques, high electrical properties based on the devices. Jaya Madhan et al. proposed junctionless TFET with schottky contacts, have polarity gate in the p + source region and source electrode near the source for n-type JTFET device. In the transfer characteristics, due to the ohmic contacts between the SE and PG the drain current increases without using the universal schottky tunneling model for Pd_2Si. However, using with UST model it maintained the same drain current. The depleted hole plasma (HP) occurred between the SE and PG interfaces which decreases the current conduction. Further, the schottky tunneling improved the current conduction. Moreover, using the schottky ohmic contact the subthreshold swing is decreased by 5.95% (59 mV/dec). Depending on the various SE type which has been controlled the threshold voltage variations [43, 55–60].

The transfer characteristics for DG-JL-TFET with schottky contact device is improved the drain current owing to the thin oxide is about t_{ox} = 1 nm and the maximum current I_{on} (21 μA/μm) and maximum I_{off} (3.15 × 10^{-13} A/μm) are observed. Further, if we increase the t_{ox}, I_{on}/I_{off} ratio will decrease. The gate dielectric materials provide the high controllability for CG (control gate) of the high dielectric constant of HfO_2, enhances the I_{on}/I_{off} ratio and gate controllability, drive current and suppress the subthreshold swing leakage current due to the reduced tunneling barrier. Which leads to an increase in the tunneling probability to flow more electrons [61].

Table 2 Work function for different gate materials

S.No	Gate Material	Workfunction	Reference
1	Hafnium	3.8, 3.9, 4.3 eV	[55–57]
2	Silicon	4.45 eV	[43]
3	Palladium	5.12 eV	[58]
4	Platinum	5.9 eV	[59]
5	Nickel	5.0 eV	[59]
6	Titanium	4.33 eV	[59]
7	Aluminum	3.9–4.2 eV	[59]

4.3 Heterostructure of STFET device

Heterostructure based FET devices offer high electron mobility, high I_{on}/I_{off} ratio,(1361–6463%) high speed, high frequency [62]. Gaurav Pande et al. published an SBTFET device incorporated with Hexagonal Boron Nitride- Encapsulated Monolayer WSe_2. The 2D thermionic emission analysis Pt-WSe_2 contacts FLP effects are measured. The thin h-BN that occurred in between the Pt and WSe_2 layer exhibits better interface resistances (in between tunnel and channel) leading to optoelectronic and spintronics applications [63].

$MoS_2/MoTe_2$ Heterostructure tunnel FET using schottky contacts has been designed using a direct bandgap. The occurred between valance band maximum and conduction band maximum simulated by density functional theory (DFT) offer better drive current. The BTBT transition exhibits negative differential transconductance in the gate overlapping position. Hence the characteristics degrade the TFET performance of the device [64].

4.4 Pocket doping of STFET devices

Pocket doping enhances the device performance to reduce the SCEs and ambipolar current. Shilpi Guin et al present about pocket doping of the SBTFET device. In the forward biasing, if the doping concentration N_p of pocket doping is minimum, the drive current will maximum current. In the reversed bias current decreases because of high resistivity to flow of electrons, to vary the length of the pocket doping L_P like 0, 1, 2, 3, 4 nm. For L_P = 2 nm offers the high current conduction of the device in the forward bias. Moreover, the reverse bias provides low current conduction due to the thick tunneling width when compared to other devices [65]. GAA Schottky Junction TFET with heavily doped device exhibits high on-current, saturation current presented absolutely and decreases the leakage current. Pocket doping aid to decrease the tunneling width and increasing electrons in the tunnel junctions due to the high electric fields [15].

5 Applications of Schottky TFET Devices

Based on the STFET characteristics the devices used in different fields such as green transistors, digital and analog, biosensor devices.

5.1 Role of Green transistor device in chemical/gas sensor

Electrostatically doped ferroelectric Schottky barrier tunnel field-effect transistor device produced by Sangeeta et al, which gives the negative perovskite ferroelectric capacitance behavior. This paves the way to improve the gate controllability, high-speed switching mechanism, limited ambipolar conduction, enhanced drive current, subthreshold, the transconductance of STFET characteristics [66]. Sebastian Glassner et al. proposed the reconfigurable nanowire with $NiSi_2$ Schottky contact and tunneling mechanism of the device exhibits the subthreshold swing below 60 mV/dec, high electrostatic controllability interface or contact regions and low ambipolar behavior with reference of three modes. Sebastian Glassner developed 3 modes A, B, C of dual gate nanowire devices. Mode A is an off-state P-type which is biased in the forward direction and a negative voltage is applied in the direction of drain to source. Mode A depicted the high on-off currents. Mode B is N-type behavior which shows high on-off ratio currents when compared to Model A. Model B is also N-type behavior but the direction only change that is a drain to the source. Mode-B gives the average on-off current ratio when compared to the other two Modes A, B. Depending on these three modes ambipolar behavior was observed. These low power, miniaturization and enhanced performance of STFET devices used in green transistor applications [67–71].

5.2 Analog and digital devices

Double pocket charge plasma Schottky barrier TFET device preventing from doping concentration problems, degradation of mobility, RDFs issues. Due to the high performance of the CP-STFET device which is used in the RF and analog circuit applications suggested by Sangeeta et al. [52, 72]. Electrostatically doped ferroelectric Schottky barrier TFET device using PZT material explained by Sangeeta Singh et al. with negative capacitance behavior. Which paves the way to intrinsic voltage amplification, high gate controllability, and negligible parasitic resistances using a simple fabrication method. Due to the FE gate stack RF FOMs parasitic enhanced and suppress the SS. Ferroelectric dopant segregated SBTFET has been explored by Puja Ghosh et al. Because of negative capacitance behaviour effect induces the electric field at tunneling junction. When the thickness of the ferroelectric is high, the memory window increases in the devices. HfO_2 offers a good memory window. As a result symmetric Fe DS-SBTFET device is used in digital inverter applications. Pocket-MSTFET explained by Qianqian Huang et al. for SoC applications. Owing to the reduced SS of about 29 mV/dec, the maximum I_{ON} current is suitable for analog and digital circuit applications [73–76].

5.3 Biosensing devices

DM-SB-TFET device explored by N.K. Hema Latha et al. exhibit high on-off current ratio with different dielectric constant and dielectric density of variations. Figure 8 represents a change of drain-source voltage, as a result, sensitivity was observed for different dielectric constants and also for different resistivity of dielectric constant K = 4. When the charge density increases the Schottky barrier become thin. This paves the way to enhance the tunneling probability and the more electrons travel from the source to channel. Moreover, sensitivity also increases. The excellent properties which pave the way to sense the charged and neutral charge biomolecules [20].DM-SE-STFET device senses both neutral and charged biomolecules. For charge density k = 10 higher electric field exists, the SB reduces and it will provide a higher drive current for the device. CP is also improved by this mechanism [77–79].

6 Responsiveness of STFET

The variation of two parameters threshold voltage and I_{ON}/I_{OFF} ratio determine the sensitivity of the biomolecules in the cavity region of the device. For neutral biomolecules, derivation becomes, [69].

$$S_{NBIO} = \frac{V_{TH(K=1)} - V_{TH(K<1)}}{V_{TH(K=1)}} \tag{1}$$

For charged biomolecules, the equation represented by

$$S_{CBIO} = \frac{V_{TH(NBIO)} - V_{TH(CBIO)}}{V_{TH(NBIO)}} \tag{2}$$

N.K. Hema Latha et al. presented dielectric modulated Schottky Barrier Tunnel Field Effect Transistor as label biosensor applications. To sense the biomolecules used suitable gate dielectric with nanogap cavity it's about source end. The tunneling rate, surface potential, electric field brought to found the sensitivity of the device for different nanogap cavity length and thickness with a variation of dielectric constant and charge density. The transfer characteristics of cavity thickness such as 2 nm, 4 nm, 6 nm and 8 nm, increase in cavity length like 5 nm, 10 nm, 15 nm, 20 nm the small variation of drive current

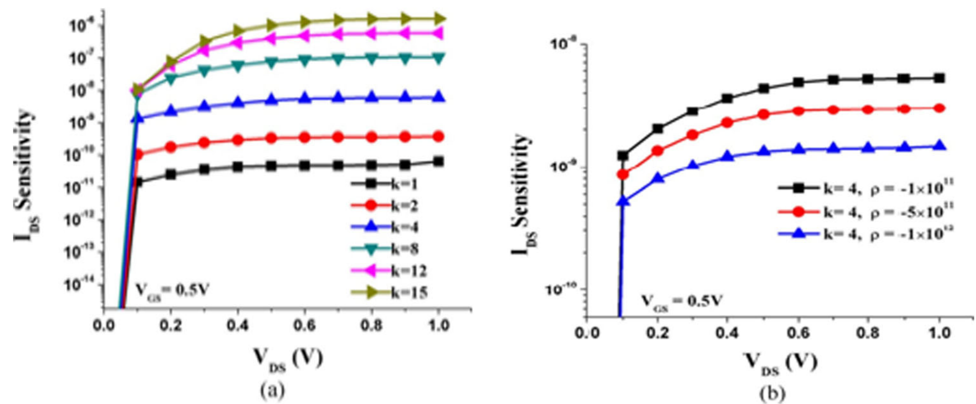

Fig. 8 Sensitivity analysis for DM-SB-TFET device at V_{GS} = 0.5 V [21]

Table 3 Dielectric constant for different biomolecules

S.No	Biomolecules	Dielectric Constant (K)	Type
1	DNA	1–64	Negatively Charge biomolecule [72, 73]
2	Streptavidin	2.1	Neutral biomolecule [74, 75]
3	Protein	2.50	Neutral biomolecule [74, 75]
4	Biotin	2.63	Neutral biomolecule [74, 75]
5	APTES	3.57	Neutral biomolecule [74, 75]

observed. For cavity thickness 4 nm and different lengths show the decreased drive current. This leads to the tunneling probability decreased. Using dielectric constant, charge density, various lengths of the cavity and thickness of the cavity found the effect of drive current. Hence characteristics are used to measure the sensitivity of the device [20].

Physically doped, charge plasma and electrically doped tunnel FET device using schottky contact. Arbita Biswas et al .compared the three different tunnel FET devices and the sensitivity is observed. For positively charged biomolecules of charge density K = 5, all the three n-TFET devices exhibit high drive current but p-TFET devices show the minimum current for the same charge density increases the tunneling probability due to the opposite charges of biomolecules because of bands are bending more at tunneling junctions. Due to maximum sensitivity for positively charged biomolecules of n-TFET devices but minimum sensitivity for p-TFET devices. Instead of using negatively charged biomolecules, as a result, low drive current was obtained for three n-TFET devices but p-TFET based devices increased in the reverse biasing. Hence, high sensitivity for negatively charged biomolecules of p-TFET but low sensitivity observed for n-TFET devices. From these three devices, the ED-DM-TFET device shows the high sensitivity [80–84].

Charge plasma Schottky contact TFET device published by Naveen Kumar et al. Gate All Around architecture assisted with doping less nanowire TFET device[85–90]. When varying the drain current with gate voltage the threshold voltage and subthreshold slope. The tunneling probability increases when the band is steepened because the conduction band is lowered at the source end of the band. Maximum transconductance was observed and a high band-to-band tunneling rate shows maximum sensitivity is observed. Transfer characteristics of the device exhibit better performance for sensitivity analysis. Therefore the planer device offers scalability, reliability, linearity to the sensing applications. Hence the dielectric constant of different biomolecules are listed in Table 3.

7 Conclusion

Semiconductor based devices are widely used in the biosensing field. The variation of dielectric constant and charge density by the change of threshold voltage leads to sense the biomolecules, viruses, etc. This review extracted the various fabrication methods with different FET devices and their performances. When compared with other FET biosensors, STFET biosensors are more sensitive depending on the electric field, surface potential, sensitivity, SS, threshold voltages parameters. The doping, pocket doping, junction-less, dielectric modulated and hetero-junction modified architectures provide excellent performances to the conventional STFET device. We also have discussed the various applications related to the conventional STFET device. Which is capable to detect small biomolecules easily when compared to other biosensor devices.

Author's Contribution All the authors are involved in the review on the schottky barrier FET device.

Data Availability There is no other data and material associated with this manuscript.

Declarations

Conflict of Interest No conflict of interest.

Consent to Participate Not applicable.

Consent for Publication Not applicable as the manuscript does not contain any data from individual.

References

1. Cheng S, Hideshima S, Kuroiwa S, Nakanishi T, Osaka T (2015) Label-free detection of tumor markers using field effect transistor (FET)-based biosensors for lung cancer diagnosis. Sensors Actuators B Chem 212:329–334. https://doi.org/10.1016/j.snb.2015.02.038
2. Wadhera T, Kakkar D, Wadhwa G, Raj B (2019) Recent advances and Progress in development of the field effect transistor biosensor: a review. J Elec Mater 48(12):7635–7646. https://doi.org/10.1007/s11664-019-07705-6
3. Sang S, Wang Y, Feng Q, Wei Y, Ji J, Zhang W (2016) Progress of new label-free techniques for biosensors: a review. Crit Rev Biotechnol 36(3):465–481. https://doi.org/10.3109/07388551.2014.991270
4. Demeke Teklemariam A, Samaddar M, Alharbi MG, Al-Hindi RR, Bhunia AK (2020) Biosensor and molecular-based methods for the detection of human coronaviruses: a review. Mol Cell Probes 54:101662. https://doi.org/10.1016/j.mcp.2020.101662
5. Syedmoradi L, Ahmadi A, Norton ML, Omidfar K (2019) A review on nanomaterial-based field effect transistor technology for biomarker detection. Microchim Acta 186(11):739. https://doi.org/10.1007/s00604-019-3850-6
6. Kumar A, Tripathi MM, Chaujar R (2019) Sub-30nm In2O5Sn gate electrode recessed channel MOSFET: a biosensor for early stage diagnostics. Vacuum 164:46–52. https://doi.org/10.1016/j.vacuum.2019.02.054
7. Buvaneswari B, Balamurugan NB (2019) 2D analytical modeling and simulation of dual material DG MOSFET for biosensing application. AEU – Int J Electron Commun 99:193–200. https://doi.org/10.1016/j.aeue.2018.11.039
8. Sadighbayan D, Hasanzadeh M, Ghafar-Zadeh E (2020) Biosensing based on field-effect transistors (FET): recent progress and challenges. TrAC Trends Anal Chem 133:116067. https://doi.org/10.1016/j.trac.2020.116067
9. Park J, Nguyen HH, Woubit A, Kim M (2014) Applications of field-effect transistor (FET)-type biosensors. Appl Sci Converg Technol 23(2):61–71. https://doi.org/10.5757/ASCT.2014.23.2.61
10. Chanda M, Dey P, De S, Sarkar CK (2015) Novel charge plasma based dielectric modulated impact ionization MOSFET as a biosensor for label-free detection. Superlattices Microstruct 86:446–455. https://doi.org/10.1016/j.spmi.2015.08.013
11. Narang R, Reddy KVS, Saxena M, Gupta RS, Gupta M (2012) A dielectric-modulated tunnel-FET-based biosensor for label-free detection: analytical modeling study and sensitivity analysis. IEEE Trans Electron Devices 59(10):2809–2817. https://doi.org/10.1109/TED.2012.2208115
12. Narang R, Saxena M, Gupta RS, Gupta M (2012) Dielectric modulated tunnel field-effect transistor—a biomolecule sensor. IEEE Electron Device Lett 33(2):266–268. https://doi.org/10.1109/LED.2011.2174024
13. Reddy NN, Panda DK (2021) A comprehensive review on tunnel field-effect transistor (TFET) based biosensors: recent advances and future prospects on device structure and sensitivity. Silicon 13(9):3085–3100. https://doi.org/10.1007/s12633-020-00657-1
14. Singh R, Kaim S, MedhaShree R, Kumar A, Kale S (2021) Dielectric engineered Schottky barrier MOSFET for biosensor applications: proposal and investigation. Silicon. https://doi.org/10.1007/s12633-021-01191-4
15. Guin S, Chattopadhyay A, Karmakar A, Mallik A (2014) Impact of a pocket doping on the device performance of a schottky tunneling field-effect transistor. IEEE Trans Electron Devices 61(7):2515–2522. https://doi.org/10.1109/TED.2014.2325068
16. Guin S, Chattopadhyay A, Karmakar A, Mallik A (2013) Influence of a Pocket Doping in a Schottky Tunneling FET. IEEE Int Futur Electron Devices:28–29. https://doi.org/10.1109/IMFEDK.2013.6602225
17. Yamamoto K, Okamoto H, Wang D, Nakashima H (2017) Fabrication of asymmetric Ge Schottky tunneling source n-channel field-effect transistor and its characterization of tunneling conduction. Mater Sci Semicond Process 70:283–287. https://doi.org/10.1016/j.mssp.2016.09.024
18. Scheller FW, Wollenberger U, Warsinke A, Lisdat F, Kim HW, Kim JP, Kim SW, Sun M-C, Kim G, Kim JH, Park E, Kim H, Park B-G (2014) Schottky Research and development in biosensors Barrier Tunnel Field-Effect Transistor using Spacer Technique. https://doi.org/10.5573/JSTS.2014.14.5.572
19. Ghosh P, Bhowmick B (2020) Effect of temperature on reliability issues of ferroelectric dopant segregated Schottky barrier tunnel field effect transistor (Fe DS-SBTFET). Silicon 12(5):1137–1144. https://doi.org/10.1007/s12633-019-00206-5
20. Latha NKH, Kale S (2020) Dielectric modulated Schottky barrier TFET for the application as label-free biosensor. Silicon 12(11):2673–2679. https://doi.org/10.1007/s12633-019-00363-7
21. Biswas A, Rajan C, Samajdar DP (2021) Sensitivity analysis of physically doped, charge plasma and electrically doped TFET biosensors. Silicon. https://doi.org/10.1007/s12633-021-01461-1
22. Ronkainen NJ, Halsall HB, Heineman WR (2010) Electrochemical biosensors. Chem Soc Rev 39(5):1747–1763
23. Scheller FW, Wollenberger U, Warsinke A, Lisdat F (2001) Research and development in biosensors. Curr Opin Biotechnol 12(1):35–40. https://doi.org/10.1016/S0958-1669(00)00169-5
24. Goode JA, Rushworth JVH, Millner PA (2015) Biosensor regeneration: a review of common techniques and outcomes. Langmuir 31(23):6267–6276. https://doi.org/10.1021/la503533g
25. Damborský P, Švitel J, Katrlík J (2016) Optical biosensors. Essays Biochem 60(1):91–100. https://doi.org/10.1042/EBC20150010
26. Falina S, Syamsul M, Rhaffor NA, Hamid SS, Zain KAM, Manaf AA, Kawarada H (2021) Ten years progress of electrical detection of heavy metal ions (HMIs) using various field-effect transistor (FET) nanosensors: A Review. https://doi.org/10.3390/bios11120478
27. Chen Y, Liu J, Yang Z, Wilkinson JS, Zhou X (2019) Optical biosensors based on refractometric sensing schemes: A review. Biosens Bioelectron 144:111693. https://doi.org/10.1016/j.bios.2019.111693
28. Alvarez M, Lechuga LM (2010) Microcantilever-based platforms as biosensing tools. Analyst 135(5):827–836. https://doi.org/10.1039/b908503n
29. Grieshaber D, MacKenzie R, Vörös J, Reimhult E (2008) Electrochemical biosensors - sensor principles and architectures. https://doi.org/10.3390/s80314000

30. Thévenot DR, Toth K, Durst RA, Wilson GS (2001) Electrochemical biosensors: recommended definitions and classification. Biosens Bioelectron 16(1–2):121–131
31. Ramos-Carrazco A, Gallardo-Cubedo JA, Vera-Marquina A, Leal-Cruz AL, Noriega JR, Zuniga-Islas C, Rojas-Hernandez AG, Gomez-Fuentes R, Berman-Mendoza D (2021) Characterization of ZnO Films Grown by Chemical Vapor Deposition as Active Layer in Pseudo-MOSFET. https://doi.org/10.1007/s11664-021-09038-9
32. Hierlemann A, Brand O, Hagleitner C, Baltes H (2003) Microfabrication techniques for chemical/biosensors. Proc IEEE 91(6):839–863
33. Rabbani S, Brishbhan P (2011) Cantilever embedded MOSFET for bio-sensing. Can Conf Electr Comput Eng:000489–000492
34. Mendiratta N, Tripathi SL (2020) A review on performance comparison of advanced MOSFET structures below 45 nm technology node. J Semicond 41(6):061401
35. Pan Y, Yin H, Huang K, Zhang Z (2019) Novel 10nm gate length MoS2 transisto fabricated on si fin substrate. https://doi.org/10.1109/JEDS.2019.2910271
36. Baptista A, Silva F, Porteiro J, Míguez J, Pinto G (2018) Sputtering physical vapour deposition (PVD) coatings: A critical review on process improvement andmarket trend demands. Coatings 8(11). https://doi.org/10.3390/coatings8110402www.mdpi.com/journal/coatings
37. Zhang Q et al (2019) Si Nanowire Biosensors Using a FinFET Fabrication Process for Real Time Monitoring Cellular Ion Actitivies. Tech Dig Int Electron Devices Meet IEDM 2018(l): 29.6.1–29.6.4
38. Saravanan M, Parthasarathy E (2021) A review of III-V Tunnel Field Effect Transistors for future ultra low power digital/analog applications. Microelectron J 114:105102. https://doi.org/10.1016/j.mejo.2021.105102
39. Lin HC et al (2015) Deep ultraviolet laser direct write for patterning sol-gel InGaZnO semiconducting micro/nanowires and improving field-effect mobility. Sci Rep 5:1–11
40. Tung CH (2013) Strained n-Channel FinFETs Featuring In Situ Doped Silicon–Carbon (Si1−yCy) Source and Drain Stressors With High Carbon Content. Digital Object Identifier. https://doi.org/10.1109/TED.2008.928025no.110
41. Chong C, Liu H, Wang S, Chen S (2021) Simulation and Performance Analysis of Dielectric Modulated Dual Source Trench Gate TFET Biosensor. Nanoscale Res Lett 16(1)
42. Wu Y, Kakushima K, Takahashi Y (2017) Formation of magnesium silicide for source material in Si based tunnel FET by annealing of Mg/Si thin film multi-stacks. In: 2017 17th International Workshop on Junction Technology (IWJT), Uji, Japan, pp. 83–84. https://doi.org/10.23919/IWJT.2017.7966522
43. Singh D, Pandey S, Nigam K, Sharma D, Yadav DS, Kondekar P (2017) A charge-plasma-based dielectric-modulated Junctionless TFET for biosensor label-free detection. IEEE Trans Electron Devices 64(1):271–278. https://doi.org/10.1109/TED.2016.2622403
44. Rajamohanan B, Pandey R, Chobpattana V, Vaz C, Gundlach D, Cheung KP, Suehle J, Stemmer S, Datta S (2015) 0.5 V supply voltage operation of in 0.65 Ga 0.35 as/GaAs 0.4 Sb 0.6 tunnel FET. IEEE Electron Device Lett 36(1):20–22. https://doi.org/10.1109/LED.2014.2368147
45. Gao A, Lu N, Wang Y, Li T (2016) Robust ultrasensitive tunneling-FET biosensor for point-of-care diagnostics. Sci Rep 6:1–9
46. Takaki R, Takemoto H, Fujikawa S, Toyoki K (2008) Fabrication of nanofins of TiO2 and other metal oxides via the surface sol-gel process and selective dry etching. Colloids Surf A Physicochem Eng Asp 321(1–3):227–232. https://doi.org/10.1016/j.colsurfa.2007.11.040
47. Pregl S, Weber WM, Nozaki D, Kunstmann J, Baraban L, Opitz J, Mikolajick T, Cuniberti G (2013) Parallel arrays of Schottky barrier nanowire field effect transistors: Nanoscopic effects for macroscopic current output. Nano Res 6(6):381–388
48. Liu Y et al (2007) Cointegration of high-performance tied-gate three-terminal FinFETs and variable threshold-voltage independent-gate four-terminal FinFETs with asymmetric gate-oxide thicknesses. IEEE Electron Device Lett 28(6):517–519. https://doi.org/10.1109/LED.2007.896898
49. Singh S, Sinha R, Kondekar PN (2016) A novel ultra steep dynamically reconfigurable electrostatically doped silicon nanowire Schottky barrier FET. Superlattice Microst 93:40–49. https://doi.org/10.1016/j.spmi.2016.02.039
50. Alabsi SS, Ahmed AY, Dennis JO, Khir MH Md, Algamili AS (2020) A review of carbon nanotubes field effect-based biosensors. https://doi.org/10.1109/ACCESS.2020.2987204
51. Singh S, Sinha R (2019) Pravin Neminath Kondekar, "impact of PZT gate-stack induced negative capacitance on analogue/RF figures-of-merits of electrostatically-doped ferroelectric Schottky-barrier tunnel FET,"IET circuits. Devices Syst 13(4):435–441. https://doi.org/10.1049/iet-cds.2018.5276
52. Singh S (2019) Sensitivity and Transient Behaviour Analysis of Electrostatically Doped Double Pocket Ferroelectric Schottky Barrier Tunnel Field Effect Transistor Using Parametric Sweep Optimization. https://doi.org/10.1166/jno.2019.2591
53. Kanungo S, Chattopadhyay S, Gupta PS, Sinha K, Rahaman H (2016) Study and analysis of the effects of SiGe source and pocket-Doped Channel on sensing performance of dielectrically modulated tunnel FET-based biosensors. IEEE Trans Electron Devices 63(6):2589–2596. https://doi.org/10.1109/TED.2016.2556081
54. Hafiz SA, Iltesha ME, Loan SA (2019) Dielectrically modulated source-engineered charge-plasma-based Schottky-FET as a label-free biosensor. IEEE Trans. Electron Devices 66(4):1905–1910. https://doi.org/10.1109/TED.2019.2896695
55. Chen S , Liu H, Wang S, Han T, Li W, Wang X (2019) A novel Ge based overlapping gate dopingless tunnel FET with high performance. https://doi.org/10.7567/1347-4065/ab3f00
56. Nigam K et al (2021) Performance and Analysis of Stack Junctionless Tunnel Field Effect Transistor. Silicon. https://doi.org/10.1007/s12633-021-00958z
57. Nigam K, Pandey S, Kondekar PN, Sharma D, Parte PK (2013) A Barrier Controlled Charge Plasma-Based TFET With Gate Engineering for Ambipolar Suppression and RF/Linearity Performance Improvement. https://doi.org/10.1109/TED.2017.2693679
58. Singh NK, Raman A, Singh S, Kumar N (2017) A novel high mobility In1-xGaxAs cylindrical-gate-nanowire FET for gas sensing application with enhanced sensitivity. Superlattice Microst 111: 518–528. https://doi.org/10.1016/j.spmi.2017.07.001
59. Li P, Zhang D, Sun Y, Chang H, Liu J, Yin N (2016) Towards intrinsic MoS2 devices for high performance arsenite sensing. Appl Phys Lett 109(6)
60. Madan J, Pandey R, Sharma R, Chaujar R (2019) Impact of metal silicide source electrode on polarity gate induced source in junctionless TFET. Appl Phys A Mater Sci Process 125(9):1–7. https://doi.org/10.1007/s00339-019-2900-6
61. Sharma P, Madan J, Pandey R, Sharma R (2021) RF analysis of double-gate Junctionless tunnel FET for wireless communication systems: a non-quasi static approach. J Electron Mater 50(1):138–154. https://doi.org/10.1007/s11664-020-08538-4
62. Pande G, Siao JY, Chen WL, Lee CJ, Sankar R, Chang YM, Chen CD, Chang WH, Chou FC, Lin MT (2020) Ultralow Schottky barriers in hexagonal boron nitride-encapsulated monolayer WSe2Tunnel field-effect transistors. ACS Appl Mater Interfaces 12(16):18667–18673. https://doi.org/10.1021/acsami.0c01025

63. Kim JH, Yang D, Chen Y, Bhattacharya P (1991) Growth and properties of InAsxSb1−x, AlyGa1−ySb, and InAsxSb1−x/AlyGa1−ySb heterostructures, vol. 111, pp. 1–5. https://doi.org/10.1016/0022-0248(91)91054-E
64. Balaji Y, Smets Q, Śzabo Á, Mascaro M, Lin D, Asselberghs I, Radu I, Luisier M, Groeseneken G (2020) MoS2/MoTe2 Heterostructure tunnel FETs using gated Schottky contacts. Adv Funct Mater 30(4):1–10. https://doi.org/10.1002/adfm.201905970
65. Bagga N, Kumar A, Bhattacharjee A, Dasgupta S (2017) Performance evaluation of a novel GAA Schottky junction (GAASJ) TFET with heavily doped pocket. Superlattice Microst 109:545–552. https://doi.org/10.1016/j.spmi.2017.05.040
66. Kumar H, Singh S, Priyadarshani KN (2021) Electrostatically Doped Schottky barrier tunnel field effect transistor. Int J Electron Lett. https://doi.org/10.1080/21681724.2021.1941282
67. Glassner S, Zeiner C, Periwal P, Baron T, Bertagnolli E, Lugstein A (2014) Multimode silicon nanowire transistors. Nano Lett 14(11):6699–6703. https://doi.org/10.1021/nl503476t
68. Huang Q et al. (2015) Comprehensive performance re-assessment of TFETs with a novel design by gate and source engineering from device/circuit perspective. Tech. Dig. - Int. Electron Devices Meet. IEDM, vol. 2015, pp. 13.3.1–13.3.4. https://doi.org/10.1109/IEDM.2014.7047044
69. Singh S, Kondekar PN, Singh AP (2017) Investigation of Analog/Radiofrequency Figures-of-Merits of Charge Plasma Schottky Barrier Tunnel Field Effect Transistor. https://doi.org/10.1166/jno.2017.2025
70. Kaur P, Buttar AS, Raj B (2021) A comprehensive analysis of nanoscale transistor based biosensor: a review. Indian J Pure Appl Phys 59:15
71. Kumar N, Raman A (2020) Low voltage charge-plasma based dopingless tunnel field effect transistor: analysis and optimization. Microsyst Technol 26(4):1343–1350. https://doi.org/10.1007/s00542-019-04666-y
72. Shin JK, Kim DS, Park HJ, Lim G (2004) Detection of DNA and protein molecules using an FET-type biosensor with gold as a gate metal. Electroanalysis 16(22):1912–1918. https://doi.org/10.1002/elan.200403080
73. Papavassiliou AG (1995) Chemical nucleases as probes for studying DNA-protein interactions. Biochem J 305(2):345–357. https://doi.org/10.1042/bj3050345
74. Vimala P, Krishna LL, Sharma SS (2021) Tfet Biosensor Simulation and Analysis for Various Biomolecules. In: Review, preprint. https://doi.org/10.21203/rs.3.rs-870076/v1
75. Wadhwa G, Raj B (2018) Label Free Detection of Biomolecules Using Charge-Plasma-Based Gate Underlap Dielectric Modulated Junctionless TFET. https://doi.org/10.1007/s11664-018-6343-1
76. Kumar P, Arif W, Bhowmick B (2016) Scaling of Dopant Segregation Schottky Barrier Using Metal Strip Buried Oxide MOSFET and its Comparison with Conventional Device. Silicon 12:811–820. https://doi.org/10.1007/s12633-016-9534-5 (Impact Factor : 0.704).SCI ISSN1876–9918
77. Kumar P, Bhowmick B (2017) 2-D analytical modeling for electrostatic potential and threshold voltage of a dual work function gate Schottky barrier MOSFET. J Comput Electron 16(3):658–665. https://doi.org/10.1007/s10825-017-1011-x
78. Kumar P, Bhowmick B (2017) 2D analytical model for surface potential based electric field and impact of wok function in DMG SB MOSFET. Superlattice Microstruct 109:805–814. https://doi.org/10.1016/j.spmi.2017.06.001
79. Kumar P, Bhowmick B (2017) A Physics Based Threshold Voltage Model for Hetero - Dielectric Dual Material Gate Schottky Barrier MOSFET. Int J Numer Model: Electron Netw Devices Fields. (Impact Factor: 0.622) 31(5)
80. Kumar P, Bhowmick B (2018) Suppression of Ambipolar Conduction and Investigation of RF Performance Characteristics of Gate Drain Underlap SiGe Schottky Barrier Field Effect Transistor. Micro Nano Lett, (Impact Factor: 1.7), ISSN: 1750–0443 2017 13(5):626–630. https://doi.org/10.1049/mnl.2017.0895
81. Kumar P, Bhowmick B (2020) Source-Drain Junction Engineering Schottky Barrier MOSFETs and their Mixed Mode Application. Silicon 12(4):821–830. https://doi.org/10.1007/s12633-019-00170-0
82. Kumar P, Bhowmick B (2018. ISSN 1555-130X) Comparative Analysis of Hetero Gate Dielectric Hetero Structure Tunnel FET and Schottky Barrier FET with n+ Pocket Doping for Suppression of Ambipolar Conduction and Improved RF/Linearity. J Nanoelectron Optoelectron 13:11
83. Kumar P, Bhowmick B, Vinod A (2019) Impact of Ferroelectric on the Electrical Characteristics of Silicon–Germanium based heterojunction Schottky Barrier MOSFET 107:257–263. https://doi.org/10.1016/j.aeue.2019.05.030 ISSN-1434-8411
84. Kumar P, Vinod A, Dharavath K, Bhowmick B (2021) Analysis and simulation of Schottky tunneling using Schottky barrier FET with 2-D analytical modeling. Silicon. https://doi.org/10.1007/s12633-020-00879-3
85. Kumar P (2021) Performance analysis of double gate dielectric modulation in Schottky FET as biomolecule sensor. Silicon. https://doi.org/10.1007/s12633-021-01197-y
86. Kale S, Kondekar PN (2017) Design and Investigation of Dielectric Engineered Dopant Segregated Schottky Barrier MOSFET With NiSi Source/Drain. IEEE Trans Electron Devices 64(11):4400–4407
87. Kale S (2019) Performance improvement and analysis of PtSi Schottky barrier p-MOSFET based on charge plasma concept for low power applications. Silicon, Springer
88. Kale S, Kondekar PN (2018) Charge Plasma Based Source/Drain Engineered Schottky Barrier MOSFET: Ambipolar Suppression and Improvement of the RF Performance. Superlattice Microstruct, Elsevier 113:799–809
89. Kale S, Kondekar PN (2016) Ferroelectric Schottky barrier tunnel FET with gate-drain underlap: proposal and investigation. Superlattice Microstruct, Elsevier 89:225–230
90. Kale S, Chandu MS (2021) Dual metal gate dielectric engineered dopant segregated Schottky barrier MOSFET with reduction in Ambipolar current. Silicon. Springer

Publisher's Note Springer Nature remains neutral with regard to jurisdictional claims in published maps and institutional affiliations.